Desalination and Water Treatment
www.deswater.com

35 (2011) 82–91
November

1944-3994/1944-3986 © 2011 Desalination Publications. All rights reserved
doi: 10/5004/dwt.2011.3134

Flat sheet MBRs: analysis of TMP rise and surface mass transfer coefficient

Robert William Field[a,*], Kaisong Zhang[b], Zhanfeng Cui[a], Byung-Kook Hwang[c]

[a]*Department of Engineering Science, Oxford University, Oxford OX1 3PJ, UK*
Tel. +44 1865 273118; Fax: +44 1865 283273; email: robert.field@eng.ox.ac.uk
[b]*Institute of Urban Environment, Chinese Academy of Sciences, Xiamen 361003, China*
[c]*Department of Environmental Engineering, Hoseo University, Asan 336795, South Korea*

Received 9 February 2011; Accepted 15 June 2011

ABSTRACT

Aeration in MBRs mitigates membrane fouling but the energy consumption for aeration is still one of the major operating costs. Two areas related to this are addressed. Firstly the reasons for the TMP jump that has been observed in certain MBRs are explored. The data is presented in terms of Resistance vs time which is considered superior to TMP vs. time. Also Resistance vs volume of permeate collected is informative. Five possible reasons for the TMP jump were suggested in 2006 and for the current data, this is reduced to the loss of connectivity/change in percolation hypothesis. Secondly data on the effect of bubble distribution on electrochemically determined surface mass transfer coefficients in an aerated flat sheet module are presented. This study particularly focuses on the effect of bubble distribution on the spatial variation of surface mass transfer with intermittent slug bubbling. This mode of operation will delay the onset of the TMP jump if biomass removal is more dependent upon maximum shear stress than mean shear stress. Two basic set-ups were considered: an orifice in the middle of the aeration tube, at the base, and two symmetrically placed orifices in the aeration tube. In the latter case the spacing between the two orifices was varied from 80–200 mm. Surface mass transfer was evaluated at 20 positions. With relatively low air rates a single orifice generates a higher average enhancement than two orifices but the reverse is found at a relatively higher air rate. The enhancement in the centre area of the module is relatively higher than that of the edge regions when using a single orifice but more uniformity was achieved with two.

Keywords: Membrane Bioreactor; Bubble distribution; Flat sheet membrane; Mass transfer; Wall shear stress; Slug bubble; TMP jump

1. Introduction

The most prevalent application of membrane processes is in the water industry with membrane bioreactors (MBR) being a fast are of growth. The technical advantages of MBRs over conventional processes are well documented and a considerable market in wastewater treatment has been achieved over the past 20 years [1,2]. The bottlenecks constraining wider deployment leading to replacement of the conventional activated sludge process (CASP) are costs and in particular the energy costs associated with aeration. Bubble induces two-phase flow and provides oxygen transfer and mass transfer in submerged MBR systems. It is well known that air bubbling provides substantial flux enhancement in membrane processes, and a considerable amount of data has been provided to demonstrate its beneficial effects in a number of model systems with different kinds of membranes [3–5].

*Corresponding author.

As other experimental and simulation studies have focused on the hydrodynamic characteristics of gas-liquid slug flow in tubes [6–9], there is a need to examine flat sheet systems. The air then rises through the rectangular channels formed between adjacent pairs of panels. For flat sheet membrane bioreactors, membrane aeration intensity is around 220 m^3/m^2h and the associated energy consumption dominates the variable cost of submerged MBR operation [10]. Even though many existing full-scale commercial MBR units operate with bubble flow, there are few publications focused on MBRs operating with intermittent injected slug flow [2]. A review on bubbling in membrane system also noted that for flat sheet membranes, few studies have been performed with air sparging in the form of slug bubbling [11]. In a previous study, we investigated the effect of bubble size and frequency on surface mass transfer in flat sheet module with single slug bubbling [12]. The results indicated that MBR operation with slug flow should reduce aeration intensity and save energy. The standard deviation of relative current enhancement at single point or small area was repeatable but the standard deviation of relative current enhancement between points was large. That study suggested that bubbles bring different hydrodynamic characteristics to different positions. In particular with the consideration of membrane fouling control in mind, spatial variations are important.

In this paper, we report on two sets of experiments. Firstly a new analysis of some already reported data, on the development of TMP with time in a MBR for three different fluxes, is presented. The second set of experiments concerned an investigation of the spatial variation of mass transfer across the whole surface when a flat sheet membrane experiences intermittent slug bubbling. An electrochemical method was used to measure the surface mass transfer coefficient at 20 positions.

2. Analysis of MBR data to ascertain probable reasons for TMP jump

2.1. Background

The TMP-time profile has been described as a three stage process [13]. Stage 1 is a short initial 'conditioning' stage that occurs over a period of a few hours and may often not be detected directly. During this stage the overall resistance becomes much greater presumably by pore blockage and closure than the initial membrane resistance. Stage 2 is a prolonged period of slow TMP rise, which Zhang et al. attributed to the accumulation of extracellular polymeric substances (EPS) and other products of bioactivity, either deposited from the bulk liquor or produced in biofilms on the membrane surface [13]. Stage 3 manifests a sudden rise in TMP. The five possible causes, which are all exacerbated by the self-accelerating nature of fouling under constant flux operation, are:

i. The inhomogeneous fouling (area loss) model;
ii. The inhomogeneous fouling (pore narrowing) model;
iii. The inhomogeneous fouling (pore loss) model;
iv. The critical suction pressure model; and
v. Changes in percolation.

These will be explained in greater detail in section 2.3.

2.2. Data

Hwang et al. made an experimental investigation of the TMP rise in MBR's and determined the microbial characteristics in the bio-cake on the membrane surface [14]. The membrane modules were all in the same MBR tank but the fluxes were different. TMP data for three fluxes, 13, 20 and 27 l/m^2 h, are given in Fig. 1.

As fluxes vary this is not illustrating the increase in resistance and therefore here a Resistance-time plot is given, in Fig. 2, using the data. Note that the end points were determined by a maximum TMP and so the end resistances are at different values of resistance. The steeper rise in stage 3 for the lowest flux is probably due to the greater amount of dead cells.

Operators of MBR plants will be interested in the change of resistance with the amount of product water produced. Fig. 3 shows the evolution of resistance in terms of resistance vs specific volume collected (l/m^2) for the three different fluxes.

The differences are shown to be more dramatic in this plot with stage 3 being particularly dramatic for the lowest flux. Furthermore the middle flux produces just as much water as the lowest flux before the terminating TMP is produced (and will have done so in a shorter time).

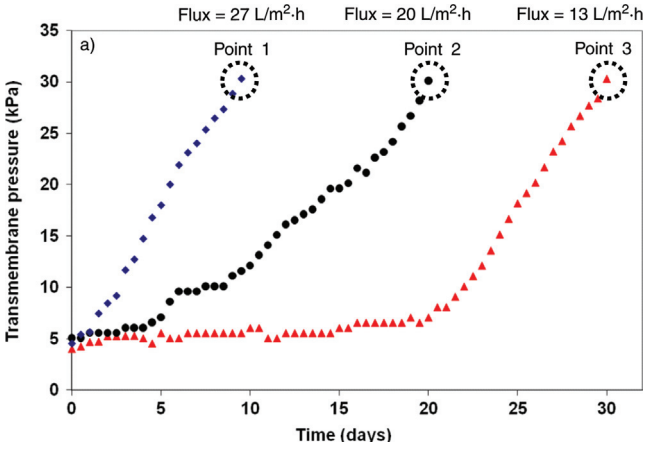

Fig. 1. TMP-time data for three different fluxes from [14].

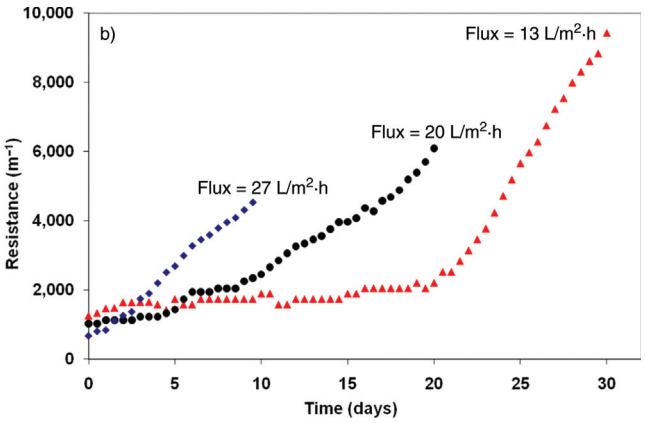

Fig. 2. Resistance-time data for three different fluxes. Note that the end points were determined by a maximum TMP.

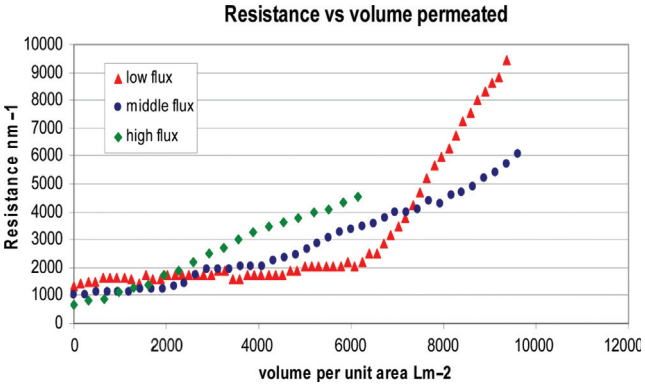

Fig. 3. Resistance-specific volume collected (L/m^2) for three different fluxes. Note that the times of operation are different.

Unlike Fig. 1, this figure definitely shows that operation at the middle flux is superior to that at the lowest one.

2.3. Analysis of TMP-time data

Paraphrasing others, it has been said that "a slow steady rise in TMP (stage 2) can be observed which eventually changes to a rapid rise in TMP (stage 3)." Viewing TMP-time plots this seems to be true (Fig. 1) for the present data but Figs. 2 and 3 show that only the rate of resistance build-up during the end of the low-flux run is very substantial. If the aim is to obtain as much water as possible before the run is terminated due to a TMP limit being reached then Fig. 3 clearly suggests that the middle flux is superior to the low one. If the stated aim is to have sustainable operation by prolonging stage 2 and avoiding stage 3, then the same conclusion is reached. This avoids the conditions that give rise to the TMP

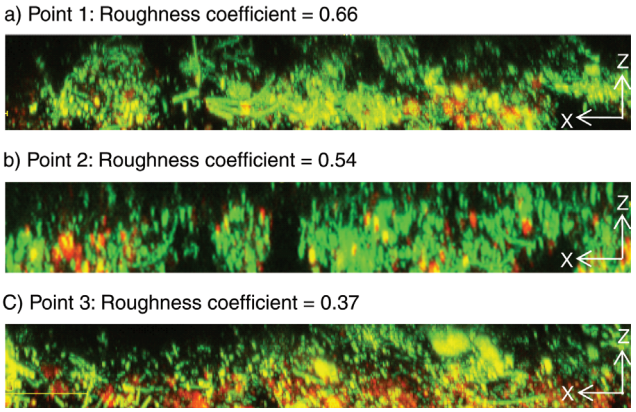

Fig. 4. CLSM images of the biocake at point 1–3 which are defined in Fig. 1. Green indicates a bacterial cell and red EPS. Roughness coefficients are output from the CLSM from [14].

jump in the low flux run. By examining Fig. 4, it is readily noted that the end of the low flux run is characterised by high EPS content next to the membrane surface. This is confirmed in Fig. 5 which shows that the maximum fraction of EPS (at a level apparently just above the membrane) is in excess of 0.4 which is double that for the other runs. The steeper rise in stage 3 for the lowest flux is probably due to the greater amount of dead cells.

2.4. Causes of the stage 3 rise

In section 2.1 the five possible mechanisms mentioned by Zhang et al. [13] were listed. References regarding the origin of these mechanisms are given therein. Our understanding of the first mechanism (inhomogeneous fouling (area loss) model) is that it is related to axial changes in permeability caused by progressive axial fouling due to slow fouling by EPS. However in the present data there is no evidence for axial changes. Indeed there seems to be no evidence for a loss of local permeability at different positions along the membrane. Clearly the second suggested mechanism (The inhomogeneous fouling (pore narrowing) model) does not apply as there were low values of membrane fouling resistance as opposed to cake resistances. Data to support this statement can be found in Hwang [14]. The third mechanism that we have discounted is mechanism (iv), the critical suction pressure model.

Examination of the profiles through the cake suggests that there has not been a collapse due to suction of the cake into/onto the membrane surface which would have occurred if this mechanism had applied.

The remaining two mechanisms are: (iii) The inhomogeneous fouling (pore loss) model, and (v) Percolation theory – sudden change in connectivity. Given that the membrane fouling resistance is relative low, as already

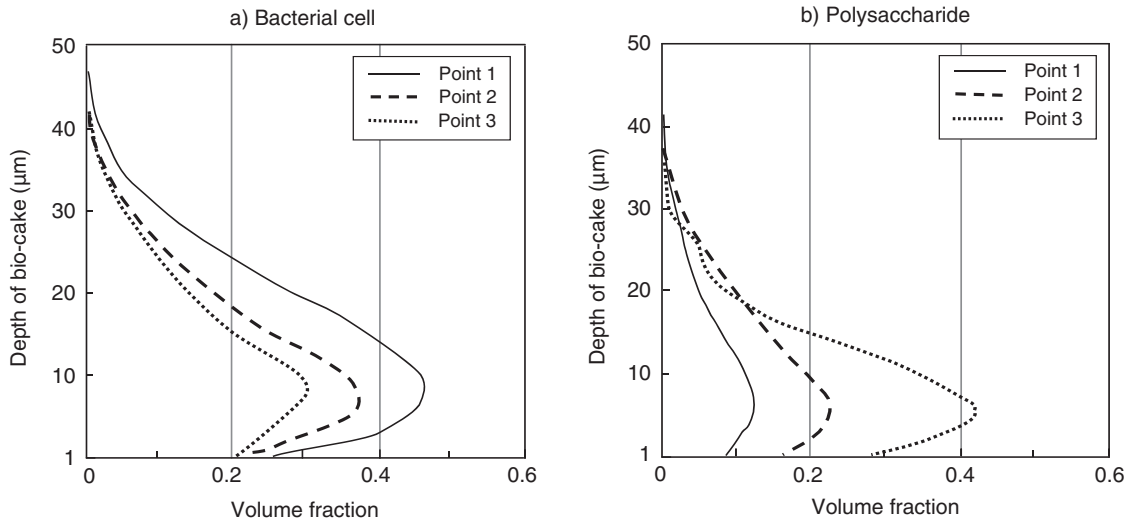

Fig. 5. Profiles through the cake at the end of each run. Note the differences in the order; in the low flux run has the fewest bacterial cells but the greatest amount of EPS.

noted, the former would seem to be an unrealistic explanation for the present data. This is especially true as the concentration of cells and EPS seems to decrease near the membrane and not increase. It is accepted that there can be some inaccuracy in CLSM measurements near the membrane surface and so the decrease maybe an artifact of the measurements. However there is no evidence of there being additional material blocking access to the pores. This leaves the sudden change in percolation due to change in connectivity. A reason is that cell death at around the 20 day mark in the low flux run led to the production of EPS and cell debris and that these small particles changed the permeability of the cake in the low flux run.

3. Materials and method for intermittent slug bubbling

3.1. Theoretical aspects

Mass transport characterization of a system can often be assessed by measuring the (convective-diffusion controlled) limiting current of a model reaction such as the reduction of ferricyanide ion to ferrocyanide ion at a cathode. From this information, transient and time-averaged mass transfer coefficients can be obtained. One electron per ion is involved:

$$Fe(CN)_6^{3-} + e^- \rightarrow Fe(CN)_6^{4-} \quad (1)$$

The reverse reaction takes place at the anode. This technique has been widely used in mass transfer coefficient measurement (e.g., see Griffith et al.) and by others (e.g., Ducom et al.) to measure the wall shear stress near a flat plate module with and without bubbles [15,16]. Further details are given in Zhang et al. but suffice to say that from the limiting current the mass transfer coefficient can be obtained [12].

Additionally one can obtain shear rate and shear stress. Following Latifi et al., quoting the work of Reiss, when circular microelectrodes are embedded in an inert wall the mass transfer coefficient, for a Newtonian fluid, is related to the mean wall velocity gradient by [17,18]:

$$k = 0.862\left(\frac{D^2\gamma}{d_e}\right)^{1/3}$$
$$F_g = V_b \quad (2)$$

where D is the diffusion coefficient of the transferred species and γ is the velocity gradient at the wall. Finally the wall shear stress can be expressed as:

$$\tau = \mu\gamma \quad (3)$$

where τ and μ represent the shear stress at the wall and the dynamic viscosity of the electrolytic solution, respectively.

3.2. Apparatus and aeration details

The experimental apparatus is shown schematically in Fig. 6. The two Perspex plates are 300 mm wide and 1000 mm high, the gap between these two flat plates is 20 mm. Microprobes were inserted to one of the surfaces and signals were collected by data logger A Canon video camera was placed in front to record visual observations. The aeration tube at the base had either a single orifice in the middle or double orifices, symmetrical placed with various gaps of 80, 120, 160 and 200 mm, between the

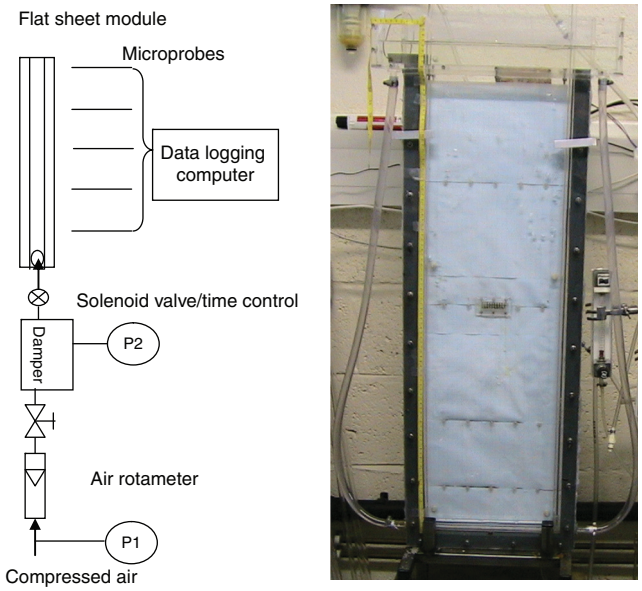

Fig. 6. The schematic draw of experiment.

holes. The orifices had a diameter of 2.0 mm; the aeration tube had a diameter of 20 mm.

Compressed air was directed to the two ends of the aeration tube through a solenoid valve with a time controller to adjust the bubbling frequency and bubble size, incorporating air flow adjustment. One orifice can induce a single slug bubble and two orifices with symmetrical distribution induced two bubbles with the same volume. The air flow rate was monitored by a rotameter upstream of a buffer tank that acted to dampen the air flow pulsation, so enabling one to read the upstream air flow rotameter easily. The solenoid valve was between the buffer tank and the module. Bubble frequency was altered by varying the time controller governing the solenoid valve. For a given pressure, the relationship between bubble volume V_b, frequency f and air flow rate F_g can be described by the flowing equation.

$$F_g = V_b$$

For a given frequency, varying the air flow rate will change the bubble volume according to the above relationship [19]. By varying bubble size and frequency, the effect on mass transfer could be identified separately. The opening time of the solenoid valve is fixed as 0.01/min. Typical values of F_g, f, V_b used in the experiment are listed in Table 1.

3.3. Experimental details

In total 20 microprobes were distributed on the surface, as shown in Fig. 7. There were four rows of 5 electrodes at the positions of 0.1 m, 0.25 m, 0.5 m, and

Table 1
Bubble size (V_b), frequency (f) and air flow rate (F_g) used in experiments

f (Hz)	F_g (ml/min)				
	V_b = 5 ml	V_b = 15 ml	V_b = 25 ml	V_b = 60 ml	V_b = 100 ml
0.167	50	150	250	600	1000

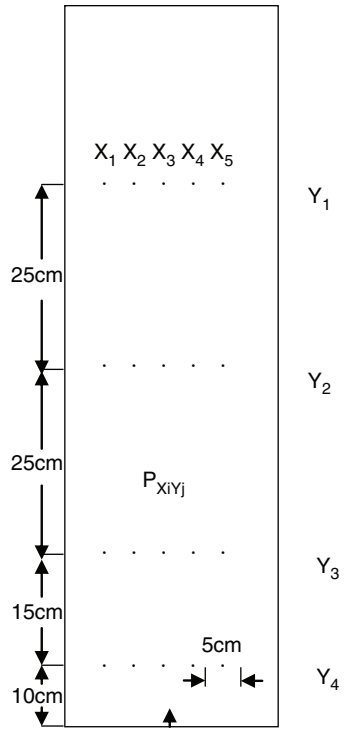

Fig. 7. Distribution of microprobes on flat sheet membrane surface. Note that there were four vertical levels and five horizontal levels.

0.75 m respectively from the aeration tube. All the experiments were performed at room temperature and the data collection at each microprobe for each particular condition lasted at least one minute. The data logger recorded the original limiting current with frequency of 100 Hz.

The electrolytic solution was a mixture of potassium ferricyanide (3 mol/m^3), potassium ferrocyanide (6 mol/m^3) and potassium chloride (0.33 mol/l^3). The potassium chloride acts as a support solution and ensures that the transfer at the cathodic surface is controlled by diffusion only. In the experiments, a constant potential difference of –400 mV was applied between the cathode (platinum microprobe with approximate diameter 0.4 mm) and the anode (stainless steel plate with the area 50 cm^2) in order to ensure limiting diffusion-controlled conditions at the microelectrodes surface (diffusional limiting plateau).

3.4. Data analysis

From the equations in Section 3.1, $I^3 \propto k^3 \propto \tau$. Thus the change of limiting current reflects the change in mass transfer coefficient and is related to the absolute value of the wall shear stress. Accurate measurement of the current and the electrode diameters (d_e) are needed to obtain mass transfer coefficient, k. In our experiment, due to the limitations of the apparatus, it was difficult to measure each electrode diameter precisely but they were roughly 0.4 mm in diameter. However the objective was to document relative enhancements and their variation and so two parameters were defined to characterize the effect of bubbling on mass transfer. In this way, the variation of the diameter of microprobes on the whole flat sheet surface could be eliminated. Here I_a is the averaged limiting current (obtained by averaging the I_i values which are the limiting current at anytime), I_{max} is the max limiting current with air bubbling, I_0 is the base limiting current without air bubbling.

1. Parameter a, the enhancement of **time-averaged** wall shear stress is $a = (I_a/I_0)^3-1$
2. Parameter b, the maximum enhancement in wall shear stress is $b = (I_{max}/I_0)^3-1$

The signal of limiting current at each microprobe was recorded independently for each particular condition, such that more than ten bubbles were recorded for the same condition. Parameter a and b are specific to each microprobe, and averaged values for the whole surface, were analysed by statistical means to yield means and standard deviations.

4. Results and discussion on intermittent slug bubbling

Firstly the results for a single orifice are given and in the next sub-section the results for the double orifices will be presented.

4.1. Single orifice bubbling

Based upon previous work the bubbling frequency was 0.167 Hz [12]. At this frequency there is little interaction between a bubble and a following bubble. The general effect of relative enhancement of 20 microprobes on the whole sheet surface with different bubble volume are shown in Fig. 8. With single bubble aeration, a volume of 60 ml was found to be optimal in maximizing both the average wall shear stress and the maximum wall shear stress enhancement. The value of a and b were averaged over the whole of the flat sheet surface. The standard deviation of average values of all points is very large indicating that different positions over the whole surface are affected differently as detailed later.

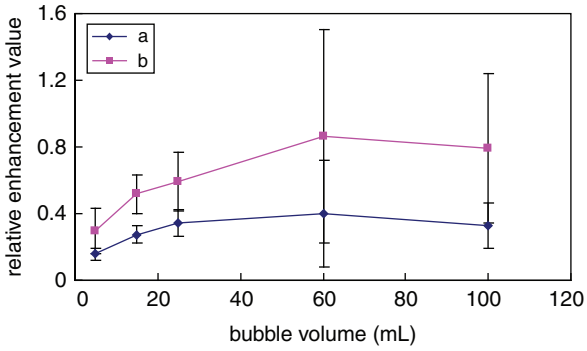

Fig. 8. General affects of bubble volume on the relative averaged wall shear stress enhancement for a bubbling frequency of 0.167 Hz.

When the injected bubble volume is small, e.g., 5 ml, the diameter of the spherical cap bubble is smaller than the gap of the flat sheet membrane. When bubble volume increases, a single bubble starts to occupy the whole cross-sectional area and at larger volumes slug bubbles are formed. Previous studies focused on hydrodynamic characteristics of upward gas-liquid slug bubble flow in vertical pipes have shown that the high velocities in the liquid film region of slug flow and the strong mixing in the elongated bubble wake cause substantial enhancement of heat transfer [6–9]. The effect in flat sheet systems was discussed by Zhang et al. [12] who showed that there exists a threshold above which enhancement is relatively insensitive to overall bubble volume. In that study a bubble volume of 60 ml was found to be optimal; this is in agreement with the result found here.

The changing pattern of relative enhancement based on the position of microprobes vs. bubble size is shown in Figs. (9a and 9b). The former summarises the data in terms of parameter a, the latter in terms of parameter b; both patterns are similar. In general, the microprobes at the centre of the whole sheet show greater enhancement. In the vertical direction (Y line), the average relative enhancement of microprobes on lines Y2 and Y3 (in the centre) are larger than those on line Y1 and Y4 (which are closer to the top and bottom respectively). With regard to horizontal positions (X lines), microprobes on lines X2 and X3 in the central surface detected a larger effect on average relative enhancement and overall X2 and X3 have relatively high values for all bubble sizes.

For single orifice bubbling in the centre, it is not surprising that more wall shear stress is induced on the central surface as revealed by the greater degree of mass transfer enhancement. This tendency is more obviously when the bubble volume is larger. Although the bubble may sway when it rises up, the probability of bubble passing through the central area is larger than it passing through the edge area and this probability increases with size, at least up to 60 ml.

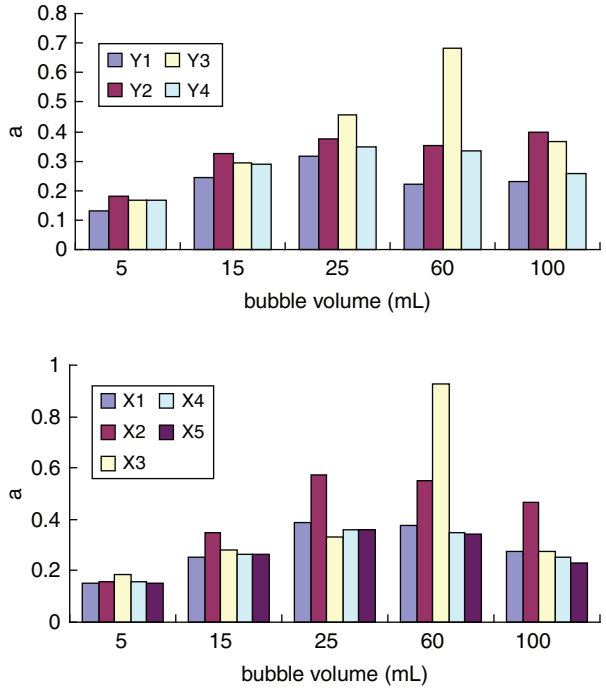

Fig. 9(a). The changing spatial pattern of relative enhancement (based on parameter a) as a function of bubble volume for a bubbling frequency of 0.167 Hz at various vertical or horizontal locations as described in the text.

4.2. Double orifice bubbling

It was found that if the periodic slug bubbling is divided between two injection points, the space between the two orifices is important. The two bubbles formed with an 80 mm spacing usually coalesce into a larger one, and so the total effect on mass transfer enhancement is very similar to that with single bubbling. For the greater spacing of 200 mm, coalescence is rare and the overall effect is very dependent upon bubble size as shown in Fig. 10. The relative enhancement induced by two-orifice bubbling compared with single orifice bubbling is shown in Fig. 10 for the same total amount of air. One interesting result is that with two bubbles, each of 12.5 ml, mass transfer average enhancement and maximum enhancement (averaged over the whole sheet surface) were poorer compared with single orifice bubbling with a total volume of 25 ml. However the total effects induced by two 30 ml bubbles were slightly superior to those induced by a single bubble with a volume of 60 ml when the spacing between the orifices was 200 mm. This position has the orifices only 50 mm from each edge with a gap of 200 mm between them.

For our experimental conditions, the bubble volume of 60 ml split between two spargers spaced 200 mm apart gave the maximum mass transfer enhancement and is probably the best choice for flux enhancement and

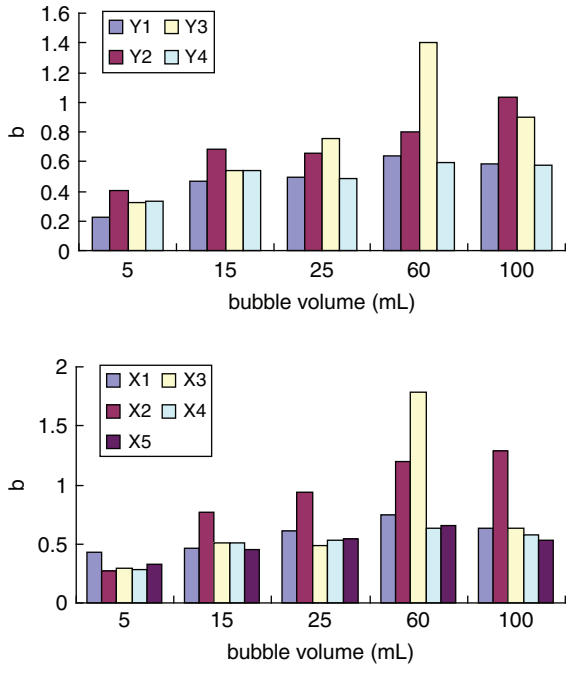

Fig. 9(b). The changing spatial pattern of relative enhancement (based on parameter b) as a function of bubble volume for a bubbling frequency of 0.167 Hz at various vertical or horizontal locations as described in the text.

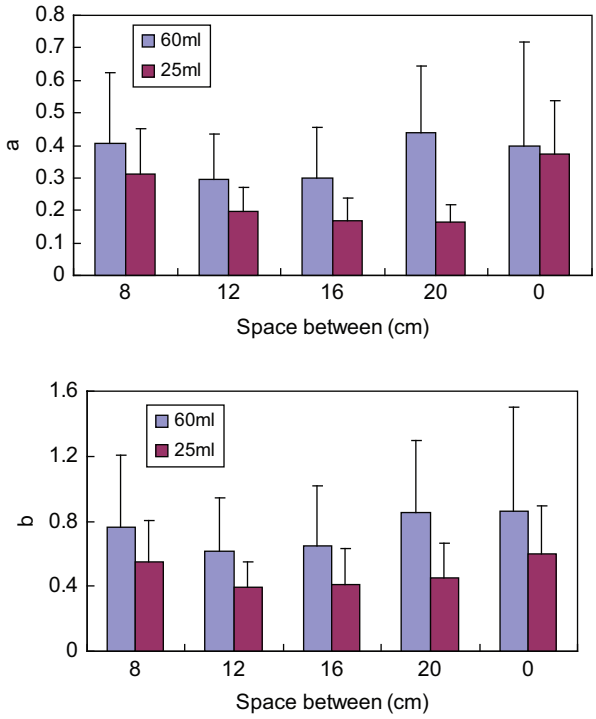

Fig. 10. General effect of spacing on the relative enhancement (space between=0 indicates single orifice in the middle of tube aeration). Frequency of bubbling: 0.167 Hz.

fouling control in actual MBRs. Whether it is better than sparging from a single orifice will depend upon the distribution of the enhancement and this is now examined.

The changing pattern of relative enhancement on the whole surface induced by two orifices with different spacings is shown in Figs. 11 and 12. When the intermittent bubble volume is either 25 ml or 60 ml, the maximum values of relative enhancements on any X or Y line was lower with two orifices compared with that induced by bubbling from a single orifice. However the average values and uniformity were improved for certain parameters. For a fixed volume of 60 ml, two isolated bubbles with 200 mm between them could induce an optimal flux enhancement and should be good for membrane fouling control. The variation of the relative enhancement in the vertical or horizontal direction should be minimized by two-orifice bubbling and Fig. 11 indicates this to a certain extent.

For a fixed total volume of 25 ml, the relative enhancement on the whole surface (including *a* and *b*) induced by two-orifice bubbling decreased significantly compared with that from a single orifice (Fig. 12). Apart from the close spacing of 80 mm, the reduction is insensitive to spacing for this bubble size.

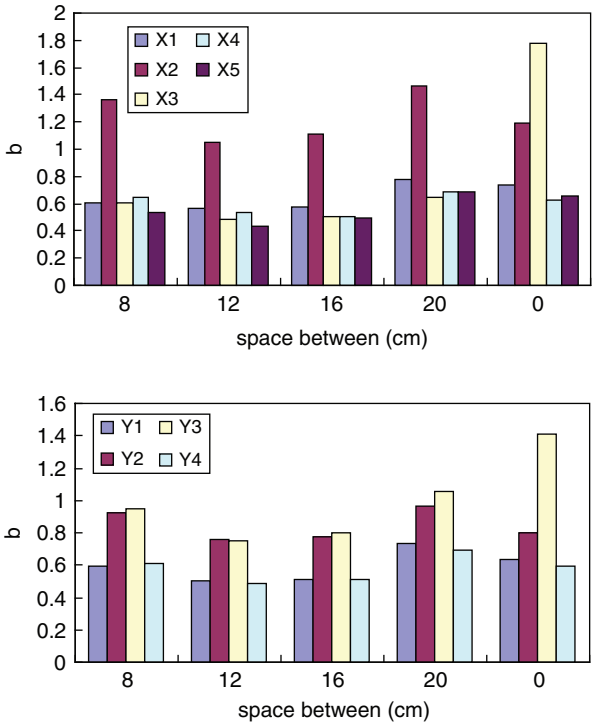

Fig. 11(b). The hydrodynamic characteristic (parameter *b*) averaged over the whole surface for an injected bubble volume of 60 ml at a bubbling frequency of 0.167 Hz.

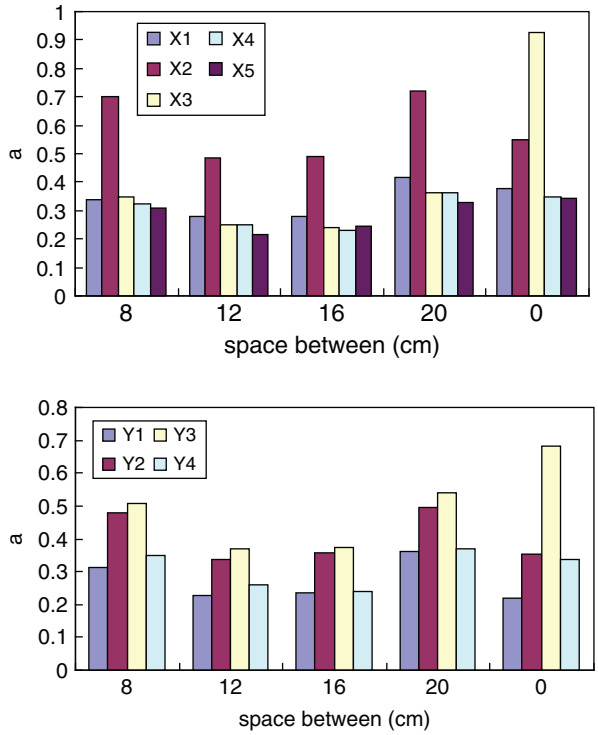

Fig. 11(a). The hydrodynamic characteristic (parameter a) averaged over the whole surface for an injected bubble volume of 60 ml at a bubbling frequency of 0.167 Hz.

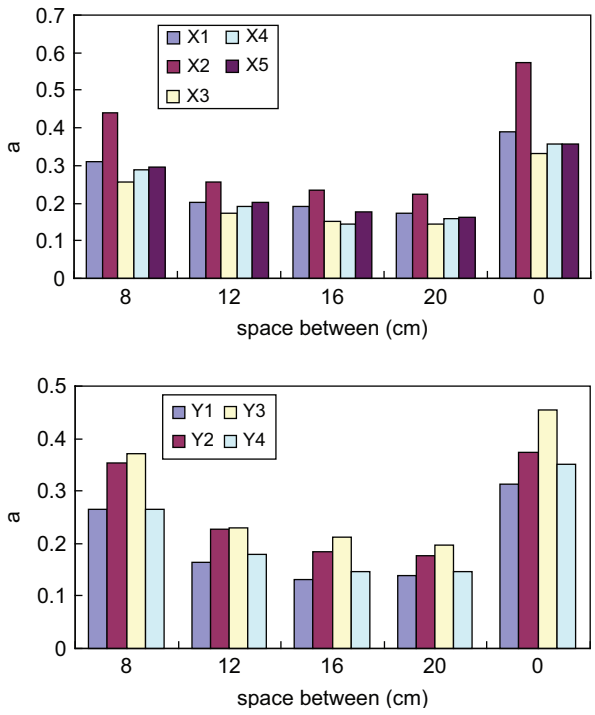

Fig. 12(a). The hydrodynamic characteristic (parameter *a*) averaged over the whole surface for an injected bubble volume of 25 ml at a bubbling frequency of 0.167 Hz.

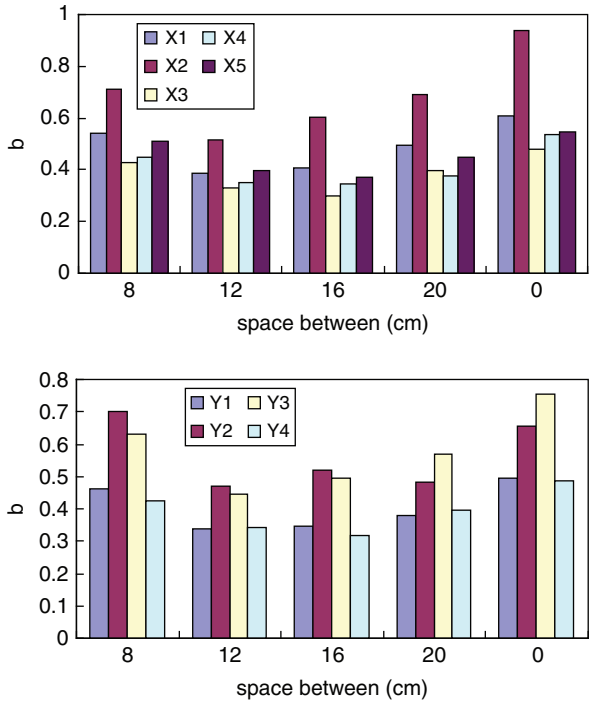

Fig. 12(b). The hydrodynamic characteristic (parameter *b*) averaged over the whole surface for injected bubble volume of 25 ml at a bubbling frequency of 0.167 Hz.

Overall, the use of a double orifice suggests that this would give better fouling controlling at the edge of flat sheet surface. For single orifice bubbling, 60 ml was optimal but the optimal size for two-orifice bubbling has yet to be determined but is probably a minimum of 60 ml. It can be anticipated that these modes of operation will delay the onset of the TMP jump if biomass removal is more dependent upon maximum shear stress than mean shear stress.

5. Conclusions

1. The MBR data suggests that the middle flux is optimal. The new presentation of Resistance vs time clearly shows that the lower flux runs end at a high value of resistance if the limit is a TMP limit. This probably makes cleaning more difficult.
2. The lower flux run ended with the EPS fraction being great than the fraction of cells. The smaller size of the former will, as is readily shown by the Carman-Kozeny equation, lead to greater cake resistance.
3. Regarding slug bubbling, with an bubble input of 25 ml every 6s (i.e., frequency of bubbling is 0.167 Hz.), single orifice bubbling is to be preferred to the use of two orifices.
4. For bubble input of 60 ml every 6s (i.e., frequency of bubbling is 0.167 Hz), the use of two orifices 50 mm from each edge (i.e., a spacing of 200 mm apart) is superior to other arrangements, partly because of the improved uniformity.
5. For a single central orifice, the total effect of the enhancement on the whole surface has been found to increase with the injected bubble volume up to an optimal value of 60 ml. The optimal value for two-orifice bubbling has yet to be determined.
6. It was found that the enhancement in the centre area is relatively higher than that of the edge area when bubbles come from a single central orifice. For two-orifice bubbling, there is greater uniformity laterally but the region between 250–500 mm from the base had higher values of enhancement.
7. If biomass removal is more dependent upon maximum shear stress than mean shear stress, periodic slug bubbling should, for fixed gas usage, delay the onset of the TMP jump.

Acknowledgements

Dr Kaisong Zhang would like to thank Chinese Academy of Sciences and National Natural Foundation of China (No. 50708090) for financial support.

References

[1] C. Visvanathan, R. Ben Aim and K. Parameswaran, Membrane separation bioreactors for wastewater treatment, Crit. Rev. Environ. Sic. Technol., 30 (2000) 1–48.
[2] S.J. Judd, P. Le-Clech, T. Taha and Z.F. Cui, Theoretical and experimental representation of a submerged membrane bioreactor system, Membr. Technol., 135 (2001) 1–9.
[3] Z.F. Cui, Experimental investigation on enhancement of crossflow ultrafiltration with air sparging, in: R. Paterson (Ed.). Effective Membrane Processes-New perspectives, Mechanical Engineering Publications Ltd., London, 1993, pp. 237–245.
[4] T.Y. Chiu and A.E. James, Critical flux enhancement in gas assisted microfiltration, J. Membr. Sci.. 281 (2006) 274–280.
[5] S.R. Smith, R.W. Field and Z.F. Cui, Predicting the performance of gas-sparged and non-gas-sparged ultrafiltration, Desalination, 191 (2006) 376–385.
[6] L. Shemer, Hydrodynamic and statistical parameters of slug flow. Int. J. Heat Fluid Flow, 24 (2003) 334–344.
[7] T.S. Mayor, A.M.F.R. Pinto and J.B.L.M. Campos, Hydrodynamics of Gas-Liquid Slug Flow along Vertical Pipes in the Laminar Regimes Experimental and Simulation Study, Ind. Eng. Chem. Res., 46 (2007) 3794–3809.
[8] D.H. Zheng and D.F. Che, Experimental study on hydrodynamic characteristics of upward gas-liquid slug flow, Int. J. Multiphase Flow, 32 (2006) 1191–1218.
[9] D.H. Zheng, X. He and D.F. Che, CFD simulations of hydrodynamic characteristics in a gas–liquid vertical upward slug flow, Int. J. Heat Mass Transfer, 50 (2007) 4151–4165.
[10] H. Fletcher, T. Mackley and S. Judd The cost of a package plant membrane bioreactor, Water Res., 41 (2007) 2627–2635.
[11] Z.F. Cui, S. Chang and A.G. Fane, The use of gas bubbling to enhance membrane processes (review), J. Membr. Sci., 221 (2003) 1–35.
[12] K.S. Zhang, Z.F. Cui and R.W. Field, Effect of bubble size and frequency on mass transfer in flat sheet MBR, J. Membr. Sci. 332 (2009) 30–37.

[13] J. Zhang, H.C. Chua, J. Zhou and A.G. Fane, Factors affecting the membrane performance in submerged membrane bioreactors, J. Membr. Sci., 284 (2006) 54–66.
[14] B.K. Hwang, W.N. Lee, K.M. Yeon, P.K. Park, C.H. Lee, I.S. Chang, A. Drews and M. Kraume, Correlating TMP increase with microbial characteristics in the bio-cake on the membrane surface in a membrane bioreactor, Environ. Sci. Technol., 42 (2008) 3963–3968.
[15] M. Griffiths, C. Ponce de Leon and F.C. Walsh, Mass transport in the rectangular channel of a filter-press electrolyzer (the FM01-LC Reactor), AIChE J., 51 (2005) 682–687.
[16] G. Ducom, F.P. Puech and C. Cabassud, Air sparging with flat sheet nanofiltration: a link between wall shear stress and flux enhancement, Desalination, 145 (2002) 97–102.
[17] M.A. Latifi, N. Midoux and A. Stock, The use of microelectrodes in the study of the flow regimes in a packed bed reactor with single phase liquid flow, Chem. Eng. Sci., 44 (1989) 2501–2508.
[18] L.P. Reiss, Investigation of Turbulence Near a Pipe Wall Using a Diffusion Controlled Electrolyte Reaction on a Circular Electrode, Ph.D. Thesis, University of Illinois, Urbana, 1962.
[19] Q.Y. Li, Z.F. Cui and D.S. Pepper, Enhancement of ultrafiltration by gas sparging with flat sheet membrane modules, Sep. Purif. Technol., 14 (1998) 79–83.